Neuron, Volume *109*

Supplemental information

The hippocampus converts dynamic entorhinal inputs into stable spatial maps

Thibault Cholvin, Thomas Hainmueller, and Marlene Bartos

Figure S1 | Mean fraction of active boutons / principal cells and mean running speed depending on the position of the animals along the tracks, related to Figure 1.

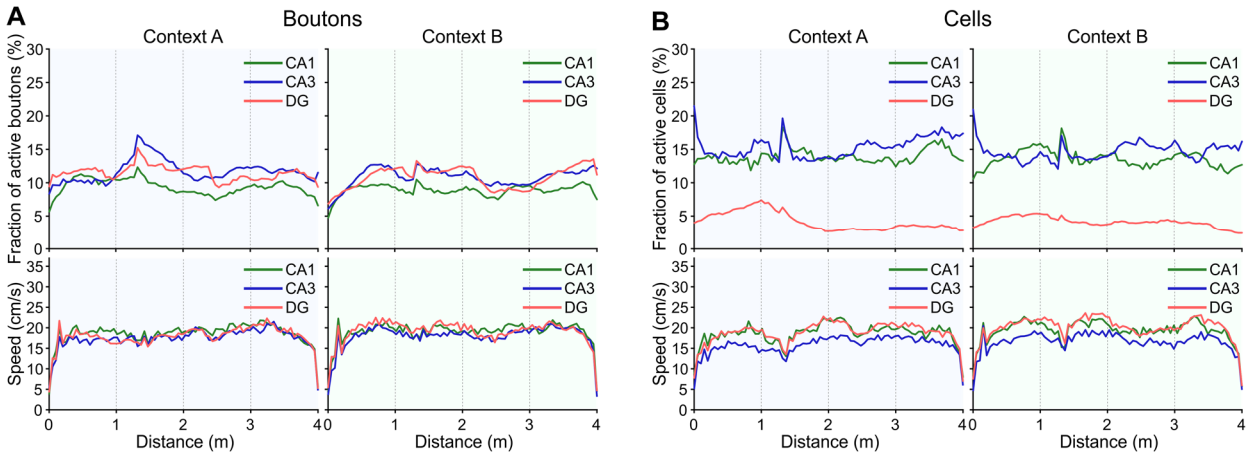

(**A**) Top panel shows the fraction of active boutons in CA1, CA3 and DG in each of the 80 bins of the two linear tracks. Bottom panel shows the mean running speed per bin in CA1, CA3 and DG boutons. Left, context A; right, context B.

(**B**) Same as **A** for hippocampal principal cells.

Figure S2 | GCaMP6s expression in the five mice in which MEC-to-Hip axonal projections were imaged, related to Figure 1.

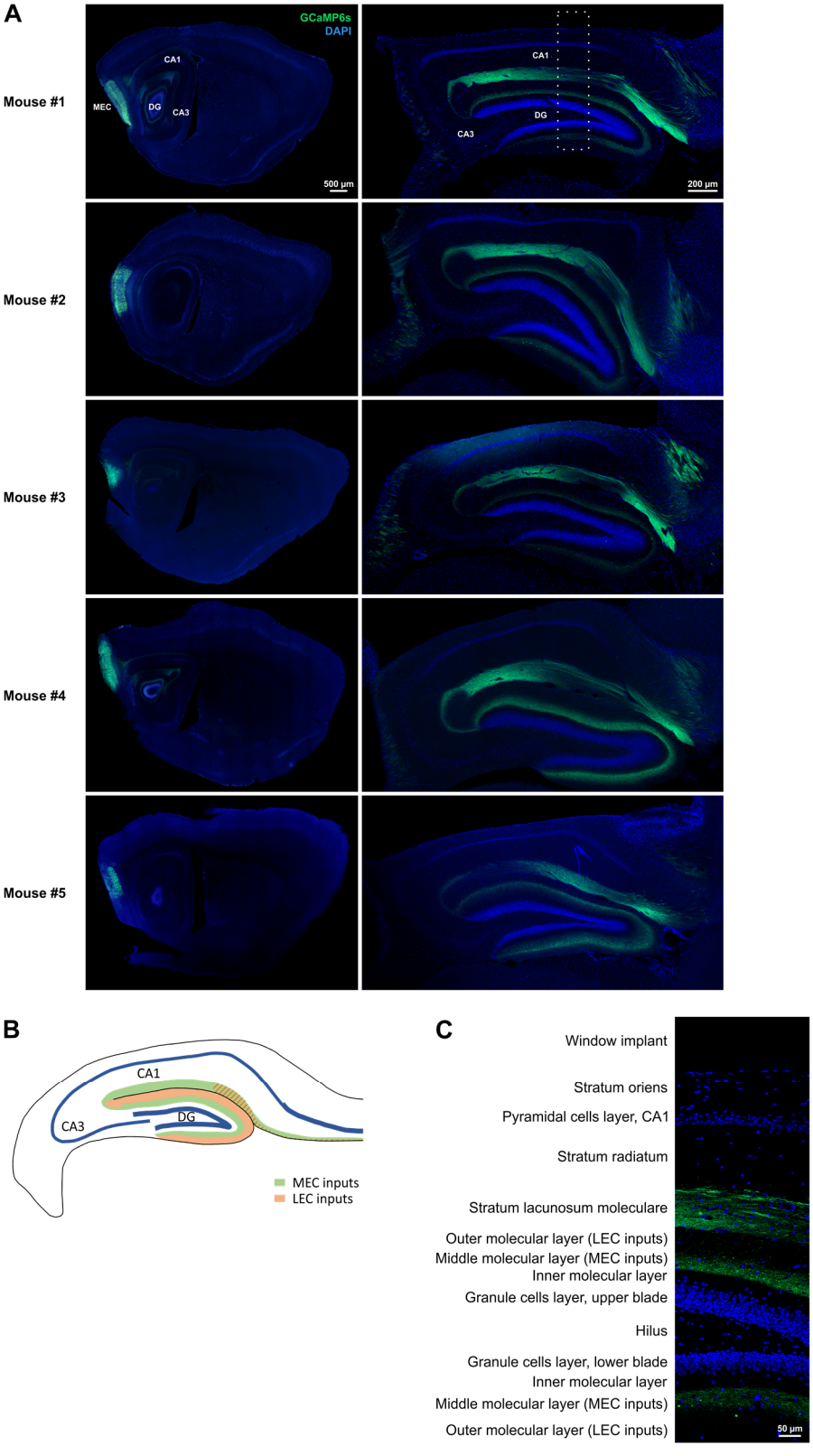

Histological verifications show GCaMP6s expression restricted to the MEC. This specificity was confirmed at the level of the hippocampus by the presence of GCaMP6s-labelled axon terminals in the middle molecular layer of the DG (where inputs from the MEC terminate) but the absence of GCaMP6s labelling in the outer molecular layer (where LEC inputs terminate).

(**A**) Left, low magnification confocal images of sagittal sections of the entire brain at the level of the MEC showing GCaMP6s infection (green). Right, MEC axonal projections to the hippocampus labeled with GCaMP6s (green). Tissue is counterstained with DAPI (blue). Each row corresponds to one animal.

(**B**) Schematic drawing of the dorsal hippocampus showing the regions in which MEC and LEC inputs terminate (in green and orange, respectively). Based on figure 10A of van Groen, T., Miettinen, P., and Kadish, I. (2003), *The Entorhinal Cortex of the Mouse: Organization of the Projection to the Hippocampal Formation,* Hippocampus 13, 133–149.

(**C**) High magnification confocal image of the area highlighted (dotted box) in **A** showing the different layers of the hippocampus, from stratum oriens of CA1 (top) to the outer molecular layer of the DG (bottom). Note how the GCaMP6s-labelled projections reaching the hippocampus are restricted to stratum lacunosum moleculare in CA1 and to the middle molecular layer in the DG, indicating that these projections are solely originating from MEC neurons.

Figure S3 | Two-photon calcium imaging of MEC boutons and hippocampal principal cells, related to Figure 1.

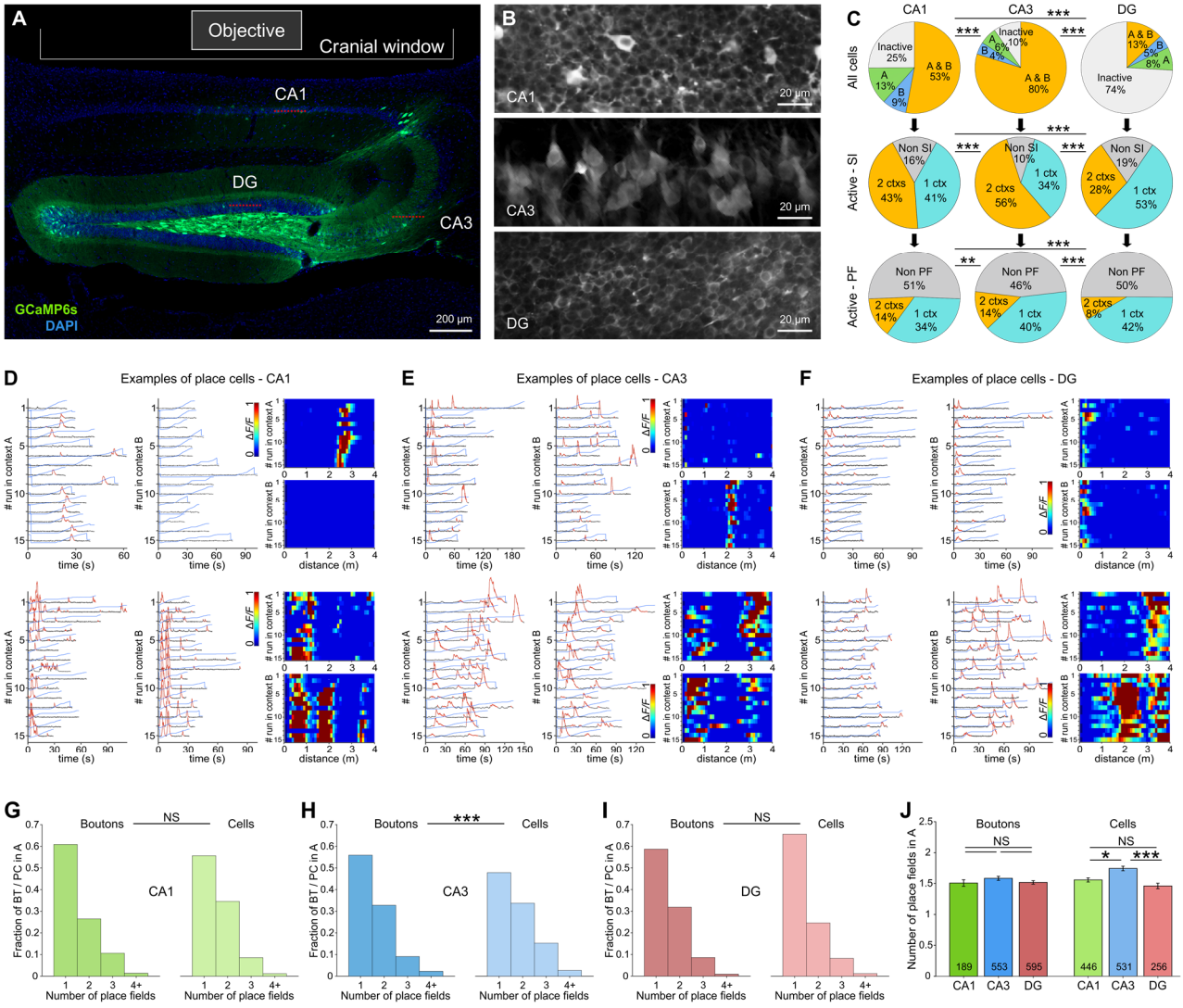

(**A**) Imaging window implantation site. Principal cells in CA1, CA3 and DG infected with GCaMP6s (green), DAPI staining in blue. Red dotted lines, imaging planes.

(**B**) Calcium activity of principal cells as imaged in CA1, CA3 and DG (see also **Videos 6-8**).

(**C**) Top row, fraction of active (> 2 transients per min) principal cells in CA1 (left), CA3 (center) and DG (right); middle row, cells showing significant spatial information; bottom row, cells with place-fields.

(**D**) Raw calcium traces (grey) with significant transients (red) and linear-track position (blue) over time of two CA1 principal cells having place-fields. Left, context A; middle, context B; right, calcium activity over track distance of the same cell. Top, context A; bottom, context B.

(**E-F**) Same as **D** for two CA3 and two DG principal cells, respectively.

(**G-I**) Distributions of the number of place-fields in context A for CA1 (**G**), CA3 (**H**) and DG (**I**) boutons and principal cells.

(**J**) Mean number of place fields in context A for all place boutons and principal cells.

C, Test for population overlap (χ^2 test). **G-I,** Rank Sum Tests, per region. **J**, ANOVA on ranks, Dunn's test, per functional domain (boutons / cells). NS, not significant; *p < 0.05; **p < 0.01; ***p < 0.001. For exact p values see **Table S1**.

Figure S4 | Imaging axon terminals of CA3 principal cells terminating in CA1 (Schaffer collaterals) provide similar results as directly imaging CA3 principal cells, related to STAR Methods.

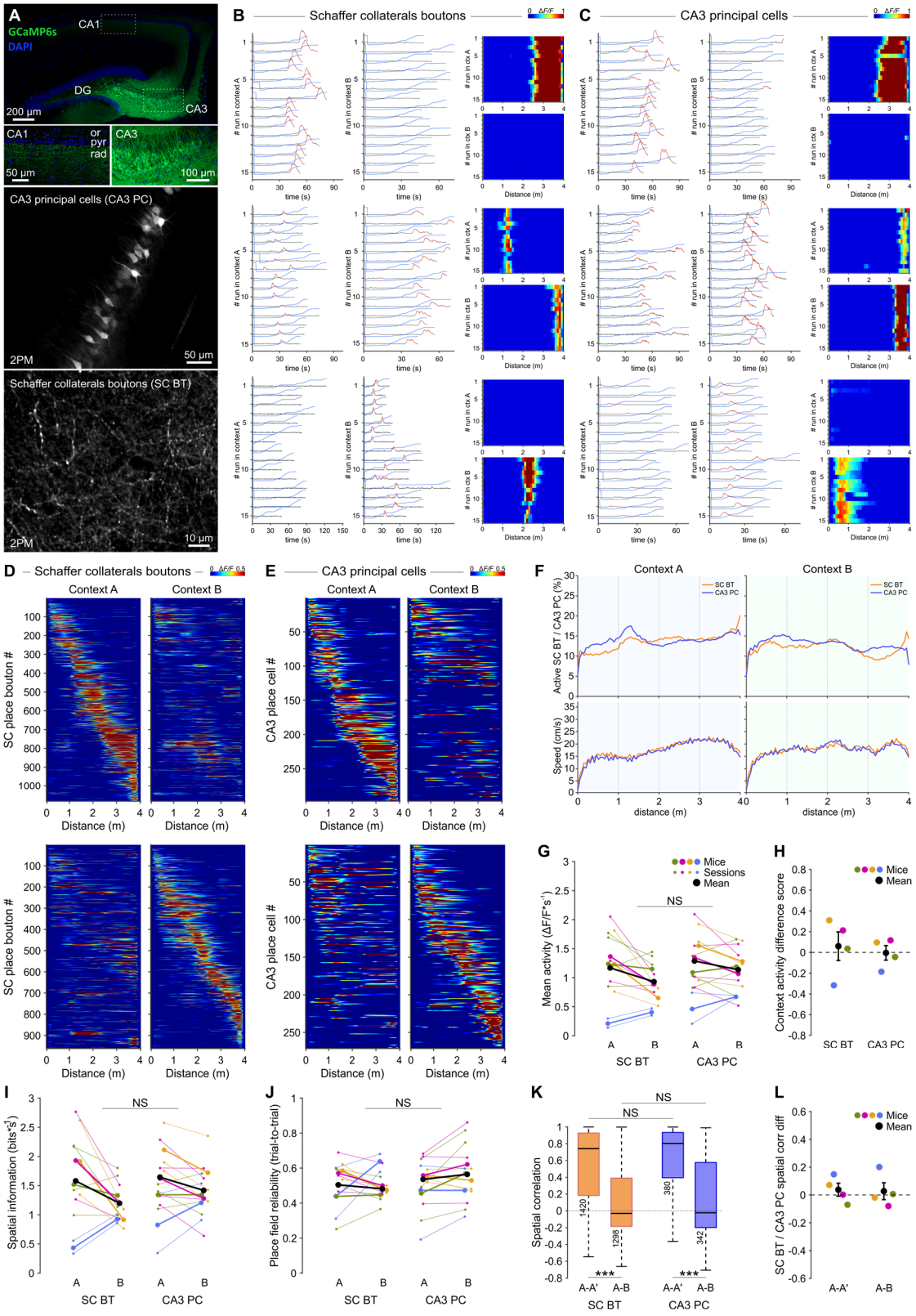

(**A**) Top panel, imaging window implantation site. Principal cells in CA3 were infected with GCaMP6s (green). DAPI staining in blue. Abbreviations: or, stratum oriens; pyr, pyramidal cell layer; rad, stratum radiatum. Center and bottom panels, calcium activity of CA3 principal cells (PC) and Schaffer collaterals boutons (SC BT) as imaged using two-photon microscopy in CA3 and CA1 (stratum radiatum), respectively.

(**B**) Raw calcium traces (grey) with significant transients (red) and linear-track position (blue) over time of three Schaffer collaterals boutons showing place fields. Left, context A; middle, context B; right, calcium activity over track distance of the same bouton. Top, context A; bottom, context B.

(**C**) Same as **B** for three CA3 principal cells showing place fields. Note that the top panels in **B** and **C** represent a bouton and a cell (respectively) which have been recorded in the same animal (albeit during separate recording sessions). The striking similarities of the activity patterns of these two units suggest that they might actually belong to the same cell, and illustrate how similar the calcium signals obtained from somata and axon terminals appeared in this experiment.

(**D**) Activity maps of place-modulated Schaffer collaterals boutons in context A (left) and context B (right). Top row, place-modulated boutons as identified in context A; bottom row, as identified in context B.

(**E**) Same as **D** for CA3 principal cells.

(**F**) Top panel, fraction of active Schaffer collaterals boutons (SC BT) and CA3 principal cells (PC) in each of the 80 bins of the two linear tracks. Low panel, mean running speed per bin in the same populations. Left, context A; right, context B.

(**G**) Mean activity ($\Delta F/F*s^{-1}$) of all Schaffer collaterals boutons (SC BT, left) and CA3 principal cells (PC, right) in both contexts (A and B). Each animal is represented by a different color. Thin lines connect data points (small dots) in contexts A and B from the same animal during a given session. Thick lines connect mean values (big dots) in contexts A and B for a given animal. Black data points and lines represent the overall mean values (n = 4 mice).

(**H**) Context activity difference score, such as $[\Delta F/F*s^{-1}_{(A)} - \Delta F/F*s^{-1}_{(B)}] / [\Delta F/F*s^{-1}_{(A)} + \Delta F/F*s^{-1}_{(B)}]$. Values above zero indicate more activity in context A, values below zero more activity in context B. Note how, at the individual (mouse) level, CA3 PC and SC BT are showing an activity bias towards the same context.

(**I**) Mean spatial information ($bits*s^{-1}$) of active (> 2 transients per min) Schaffer collaterals boutons (SC BT, left) and CA3 principal cells (CA3 PC, right) in both contexts (A and B).

(**J**) Mean trial-to-trial reliability of place-modulated Schaffer collaterals boutons (SC BT, left) and CA3 principal cells (CA3 PC, right) in both contexts (A and B).

(**K**) Mean activity correlations between first and second blocks of runs in the first context (A-A') and between the first block of runs in context A and the first block of runs in context B (A-B) for place-modulated Schaffer collateral boutons (SC BT, left) and CA3 principal cells (CA3 PC, right).

(**L**) Spatial correlation difference between place-modulated Schaffer collaterals boutons and CA3 principal cells [$Corr_{(SC\ BT)} - Corr_{(CA3\ PC)}$], for the first and second blocks of runs in the first context (A-A', left) and for the first block of runs in context A and the first block of runs in context B (A-B, right).

G, I, J, Two-Way Repeated Measures ANOVA. **K**, ANOVA on ranks, Dunn's test. NS, not significant; ***p < 0.001. For exact p values see **Table S1**.

Figure S5 | Characterization of the baseline noise, peak amplitude and kinetic properties of calcium transients recorded at axon terminals of CA3 principal cells terminating in CA1 (Schaffer collaterals) as compared to CA3 principal cell somata, related to Figure S4.

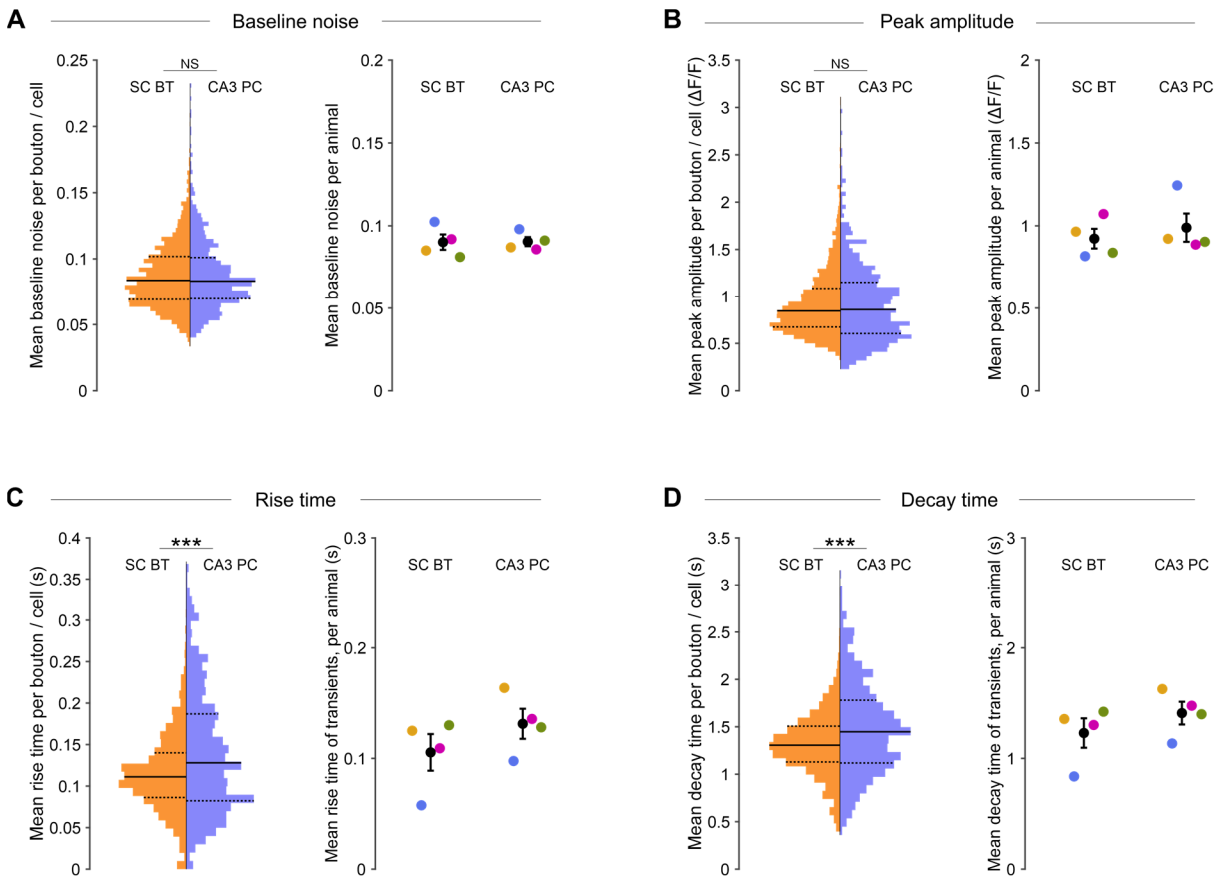

(A) Mean baseline noise of individual Schaffer collateral boutons (SC BT) and CA3 principal cell somata (CA3 PC). Baseline noise is defined as the coefficient of variation of the baseline fluorescence (fluorescence signal without significant calcium transients).

(B) Mean peak amplitude of significant transients of individual SC BTs and CA3 PCs. Transients were averaged and peak amplitude determined for each SC BT and CA3 PC (see **STAR Methods**).

(C) Mean rise time of averaged significant transients obtained from individual SC BTs and CA3 PCs. Rise time is defined as the time in which the amplitude rises to $1\text{-}e^{-1}$ (~0.63) of the peak amplitude.

(D) Mean decay time of averaged significant transients obtained from individual SC BTs and CA3 PCs. The decay time is defined as the time in which the amplitude decays to e^{-1} (~0.37) of the peak amplitude.

A-D, Left, data per bouton / cell; right, data per animal (each animal is represented by a different color, and black data points represent the overall mean values ± SEM (n = 4 mice)). Left, Rank Sum-Tests, NS, not significant; ***p < 0.001. For exact p values see **Table S1**.

Figure S6 | MEC bouton activity and spatial information are similar in both contexts, related to Figures 1 and S3.

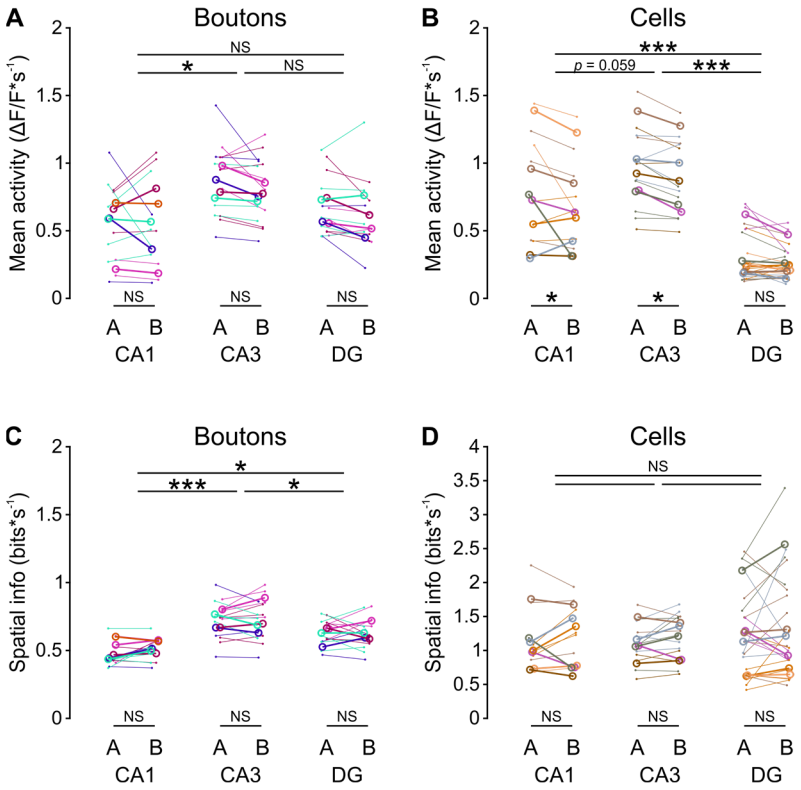

(**A**) Mean activity ($\Delta F/F*s^{-1}$) of all MEC boutons in CA1, CA3 and DG, in both contexts (A and B).

(**B**) Same as **A** for all hippocampal principal cells.

(**C**) Mean spatial information ($bits*s^{-1}$) of active (> 2 transients per min) boutons in CA1, CA3 and DG, in both contexts (A and B).

(**D**) Same as **C** for active hippocampal principal cells.

A-D, each animal is represented by a different color. Thin lines connect data points (small dots) in contexts A and B from the same animal during a given session. Thick lines connect mean values (circles) in contexts A and B for a given animal. Two-Way Repeated Measures ANOVA, Tukey post-hoc test. NS, not significant; *p < 0.05; ***p < 0.001. For exact p values see **Table S1**.

Figure S7 | MEC boutons showing grid-like activity patterns represent between one quarter (in CA1 and DG) and one third (in CA3) of the boutons having at least one place field, related to Figure 1.

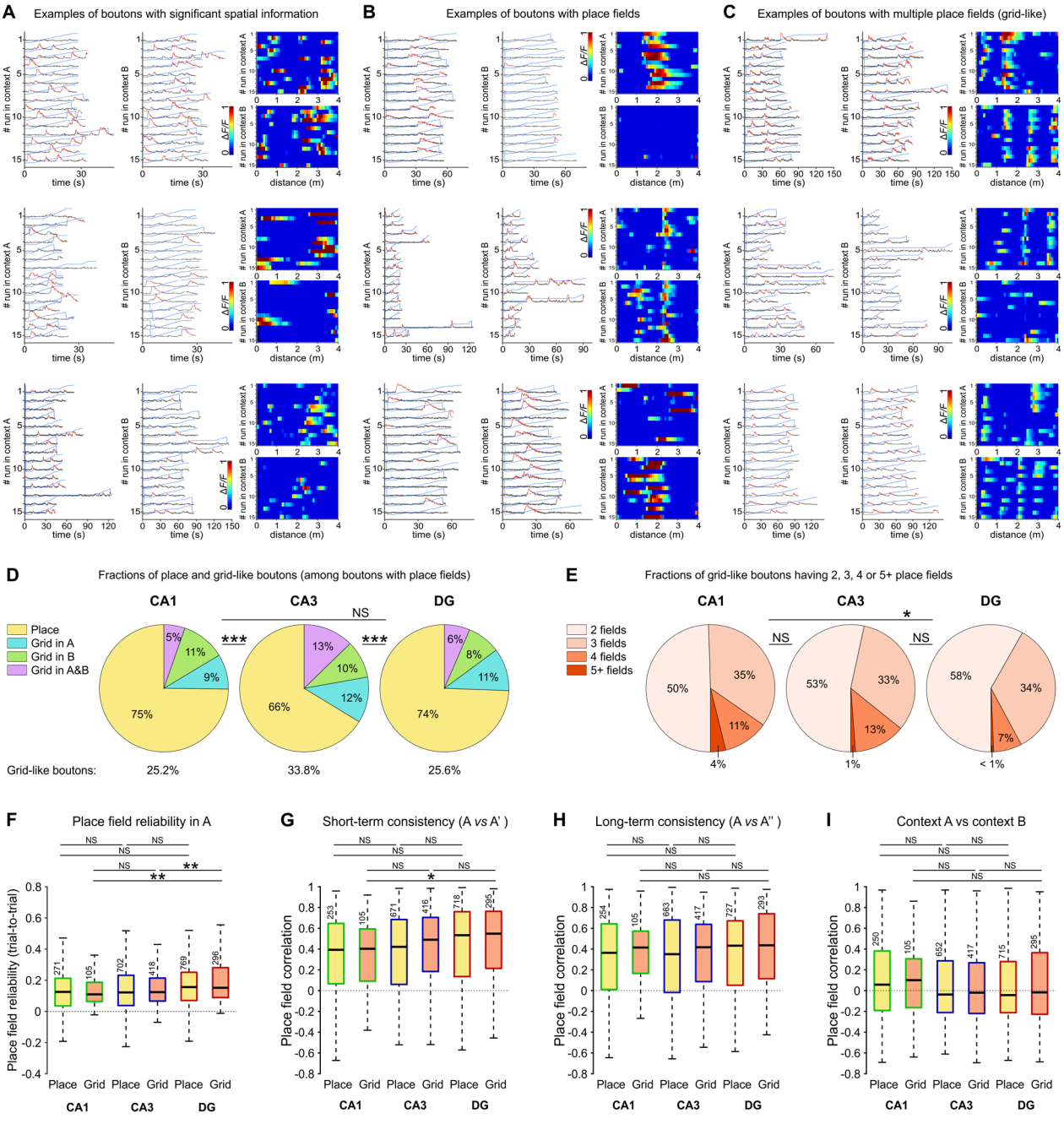

(**A**) Raw calcium traces (grey) with significant transients (red) and linear-track position (blue) over time of three boutons showing significant spatial information. Left, context A; middle, context B; right, calcium activity over track distance of the same bouton; top, context A; bottom, context B.

(**B-C**) Same as **A** for three boutons having place fields (**B**) and three boutons showing multiple place fields organized in grid-like patterns (**C**).

(**D**) Fractions of boutons showing grid-like patterns in context A, context B, or both contexts among boutons having place fields (see Methods) in CA1 (left), CA3 (center) and DG (right).

(**E**) Distribution of the grid-like boutons depending on their maximal number of place fields (in either context) in CA1 (left), CA3 (center) and DG (right).

(**F**) Mean trial-to-trial reliability of place and grid-like boutons in context A.

(**G**) Mean activity correlations between first and second blocks of runs in context A (A-A') for place and grid-like boutons.

(**H**) Mean activity correlations between first and third blocks of runs in context A (A-A'') for place and grid-like boutons.

(**I**) Mean activity correlations between all runs in contexts A and B for place and grid-like boutons.

D-E, tests for population overlap ($\chi 2$ test). **F-I**, ANOVA on ranks, Dunn's test. NS, not significant; *$p < 0.05$; **$p < 0.01$; ***$p < 0.001$. For exact p values see **Table S1**.

Figure S8 | Retrograde tracing reveals different cell populations in layers II and III of the medial entorhinal cortex (MEC) projecting to CA1, CA3 and DG hippocampal areas, related to Figure 1.

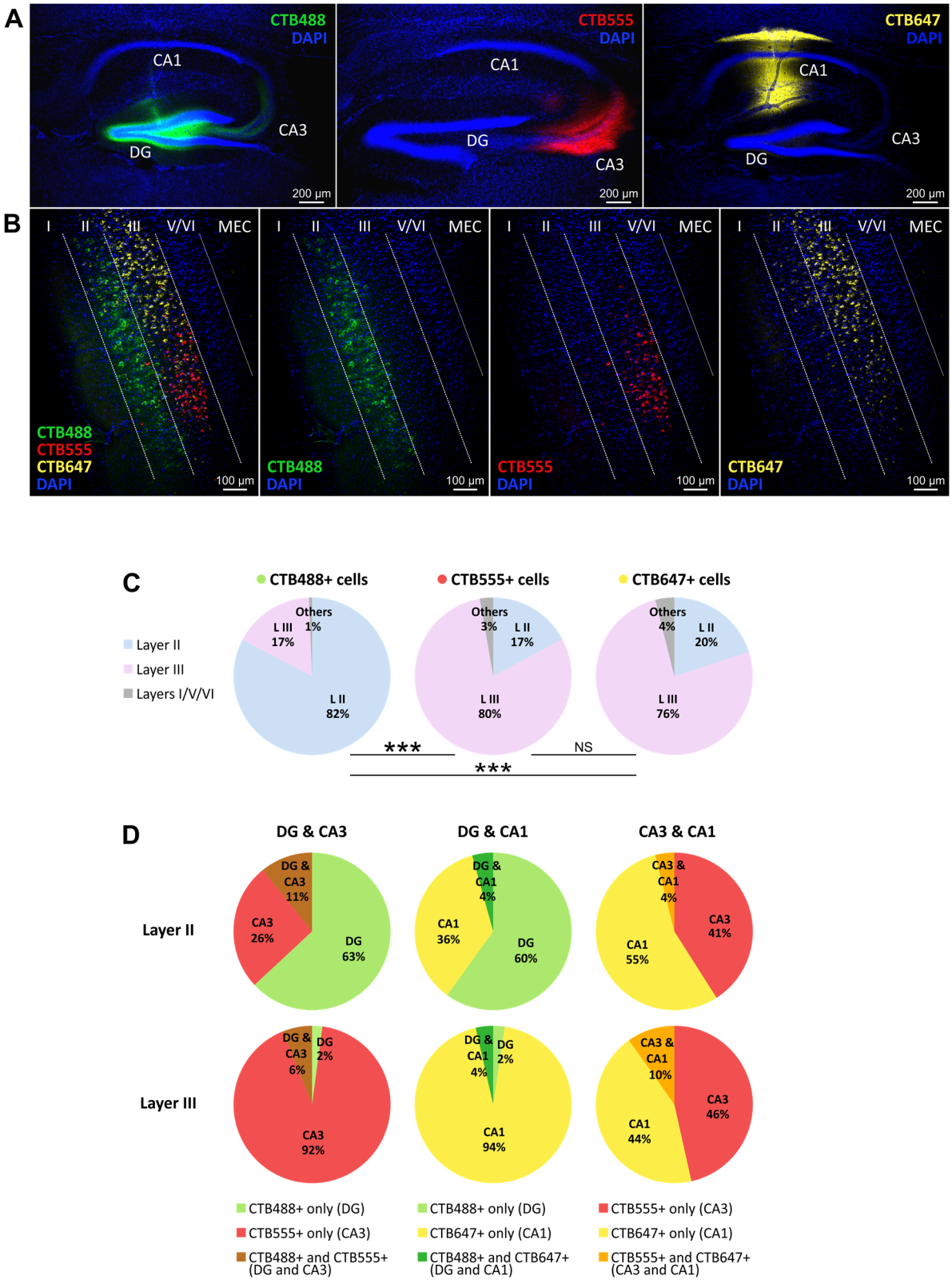

(**A**) Confocal images showing the specificity of the injection sites of the retrograde tracers cholera toxin subunit B (CTB) conjugated with Alexa Fluor 488 (green), 555 (red) or 647 (blue) in the DG, CA3 and CA1, respectively (see **STAR Methods,** n = 6 mice).

(**B**) Confocal images showing MEC cells projecting to the DG (green), to CA3 (red) and to CA1 (blue). Dotted white lines indicate the borders of the cortical layers, delineated based on DAPI staining (blue).

(**C**) Proportions of MEC cells labelled with CTB488 (and thus projecting to the DG, left), CTB555 (projecting to CA3, center) or CTB647 (projecting to CA1, right) depending on the cortical layer in which they reside. Note the striking difference between DG-projecting MEC cells (mainly located in layer II) and CA1- and CA3-projecting MEC cells (mainly located in layer III).

(**D**) Left, proportions of MEC cells retrogradely labelled with CTB488, CTB555 or both tracers (and thus projecting to the DG, CA3 or both hippocampal areas) in layer II (top) and layer III (bottom) of the MEC. Center, proportions of MEC cells retrogradely labelled with CTB488, CTB647 or both tracers (and thus projecting to the DG, CA1 or both hippocampal areas); right, proportions of MEC cells retrogradely labelled with CTB555, CTB647 or both tracers (and thus projecting to CA3, CA1 or both hippocampal areas).

C, tests for population overlap ($\chi 2$ test). NS, not significant; ***$p < 0.001$. For exact p values see **Table S1**.

Figure S9 | MEC boutons with a place-field show low reliability over multiple exposures to the same context (similar to Figure 2, for context B), related to Figure 2.

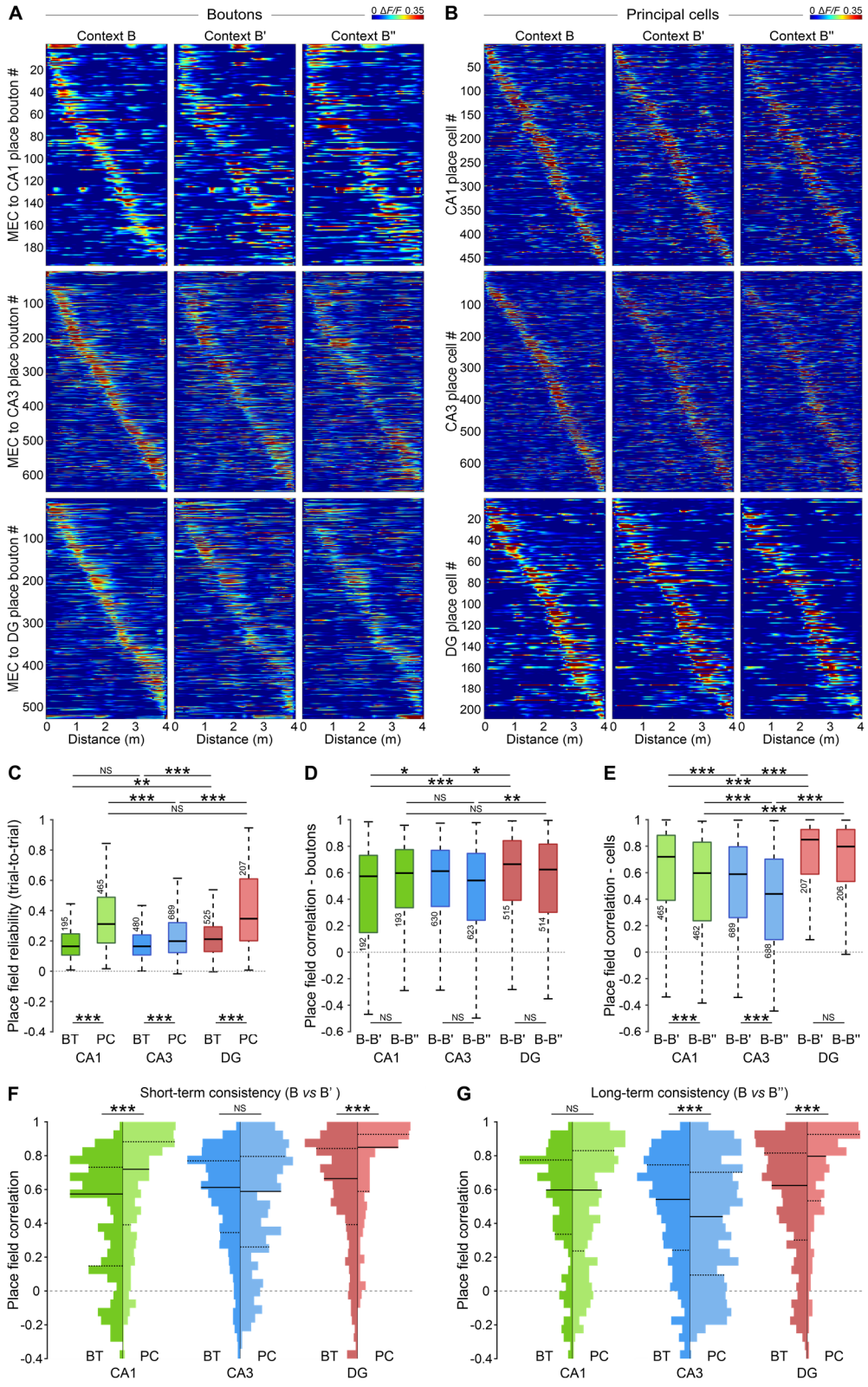

(**A**) Activity maps of MEC-to-CA1 (top), -CA3 (middle) or -DG (bottom) place-modulated boutons during the first (left), second (middle) and third (right) blocks of runs in context B.

(**B**) Same as **A** for principal cells (PC) in CA1, CA3 and DG, respectively.

(**C**) Mean trial-to-trial reliability of place boutons (BT) and PC responses in context B.

(**D**) Mean activity correlations between first and second blocks (A-A') and first and third blocks (A-A'') for place BT on consecutive runs.

(**E**) Same as **D** for PC.

(**F**) Mean activity correlations between first and second blocks of runs in context B; comparison between place BT and PC for each region.

(**G**) Same as **F** for the first and third blocks of runs.

C-E, ANOVA on ranks, Dunn's test. **F-G,** Rank Sum-Tests, per region (CA1 / CA3 / DG). Values represent number of BTs / PCs. Boxes, 25th to 75th percentiles; bars, median; whiskers, 99% range. NS, not significant; *$p < 0.05$; **$p < 0.01$; ***$p < 0.001$. For exact p values see **Table S1**.

Figure S10 | Complementary analyses on place field correlations between blocks of runs in MEC boutons and hippocampal cells, related to Figures 2 and S9.

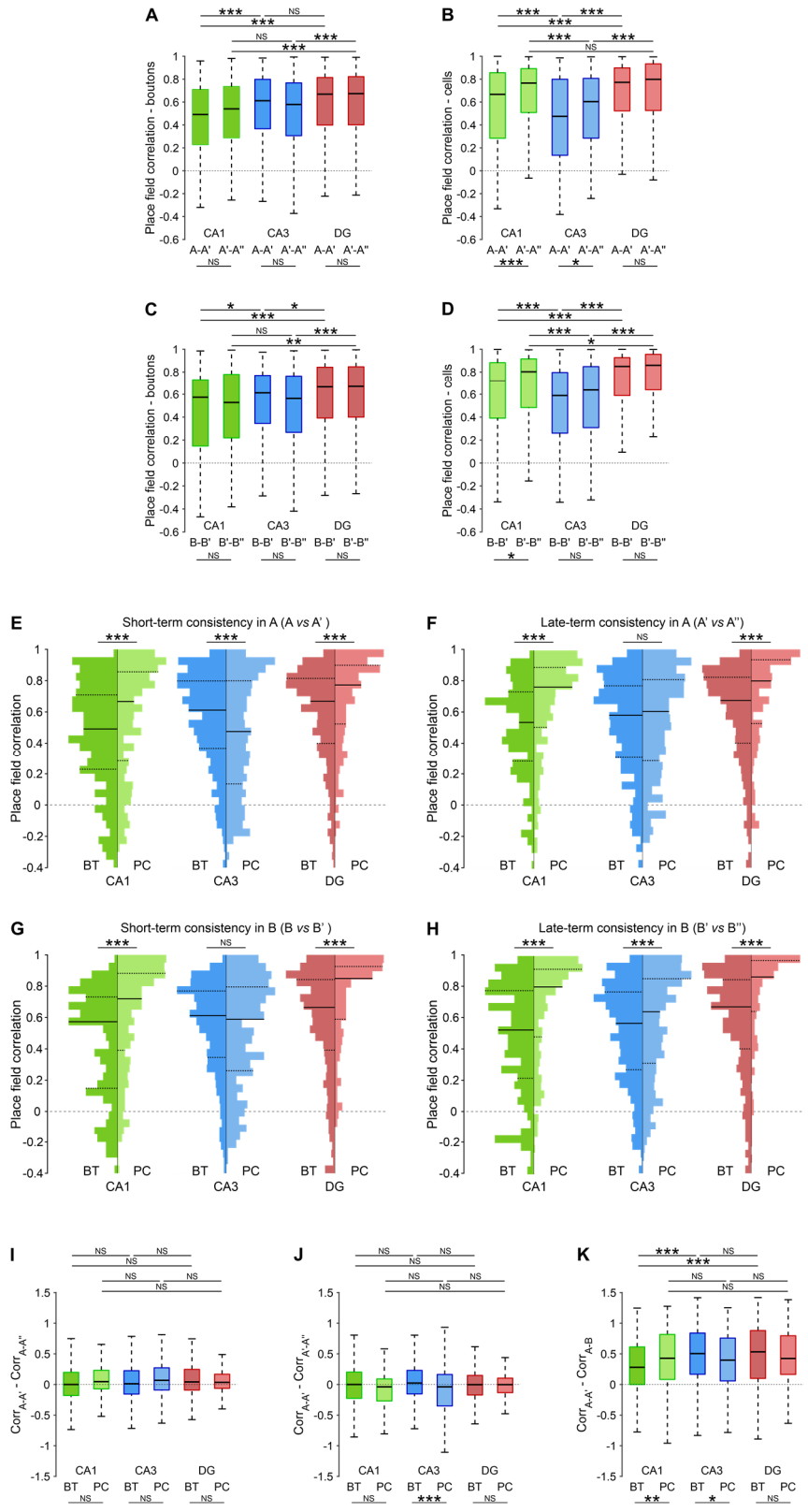

(**A**) Mean activity correlations between first and second blocks (A-A', short-term consistency) and second and third blocks (A'-A'', late-term consistency) of subsequent runs in context A for boutons (BTs) with place field(s).

(**B**) Same as **A** for principal cells (PCs) with place field(s).

(**C**) Mean activity correlations between first and second blocks (B-B', short-term consistency) and second and third blocks (B'-B'', late-term consistency) in context B for BTs with place field(s).

(**D**) Same as **C** for PCs with place field(s).

(**E**) Mean activity correlations between first (A) and second (A') blocks of runs in context A; comparison between MEC BTs and PCs with place field(s) for each hippocampal region (same data as in Figure 2F).

(**F**) Same as **E** but with place field correlations between the second (A') and third (A'') blocks of subsequent runs in context A.

(**G**) Mean activity correlations between first (B) and second (B') blocks of runs in context B; comparison between MEC BTs and PCs with place field(s) for each hippocampal region.

(**H**) Similar to **G** but between second (B') and third (B'') blocks of runs in context B.

(**I**) Effect size (delta, i.e. difference) of the mean activity correlations between first and second blocks (A-A') and first and third blocks (A-A'') of runs in context A for MEC BTs and hippocampal PCs with place field(s) for all three hippocampal areas.

(**J**) Effect size of the mean activity correlations between first and second blocks (A-A') and second and third blocks (A'-A'') of runs in context A for place MEC BTs and PCs in the three hippocampal regions. Note similar effect sizes between areas indicating similar changes in stability of place field correlations across sessions.

(**K**) Effect size of the mean activity correlations between first and second blocks of runs in context A (A-A') and the first block of runs in context A vs the first block of runs in context B (A-B) for MEC BTs and hippocampal PCs with place field(s). Note that the mean remapping between contexts compared to short-term stability of place fields is comparable among hippocampal areas, with a mildly higher mean effect size for CA1 PCs compared to CA1 MEC boutons ($p < 0.001$), similar effect size for DG ($p = 0.31$) and a lower one for CA3 PCs compared to their MEC boutons ($p < 0.05$).

A-D and I-K, ANOVA on ranks, Dunn's test. Boxes, 25th to 75th percentiles; bars, median; whiskers, 99% range. **E-H**, Rank Sum-Tests, per region (CA1 / CA3 / DG). NS, not significant; *p < 0.05; **p < 0.01; ***p < 0.001. For exact p values see **Table S1**.

Figure S11 | Removal of putative duplicates: methodology (A-C) and comparison between the results obtained using the full datasets (D, F) and after removal of putative duplicates (E, G), related to Figures 1-3 and STAR Methods.

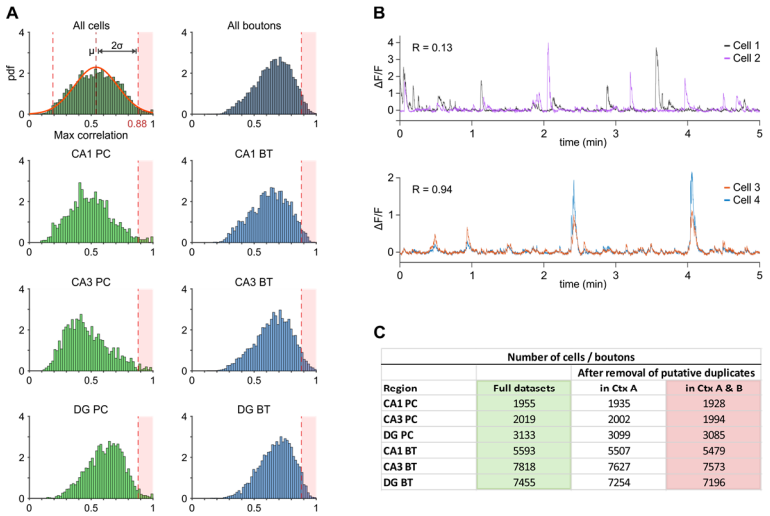

C

Number of cells / boutons			
		After removal of putative duplicates	
Region	Full datasets	in Ctx A	in Ctx A & B
CA1 PC	1955	1935	1928
CA3 PC	2019	2002	1994
DG PC	3133	3099	3085
CA1 BT	5593	5507	5479
CA3 BT	7818	7627	7573
DG BT	7455	7254	7196

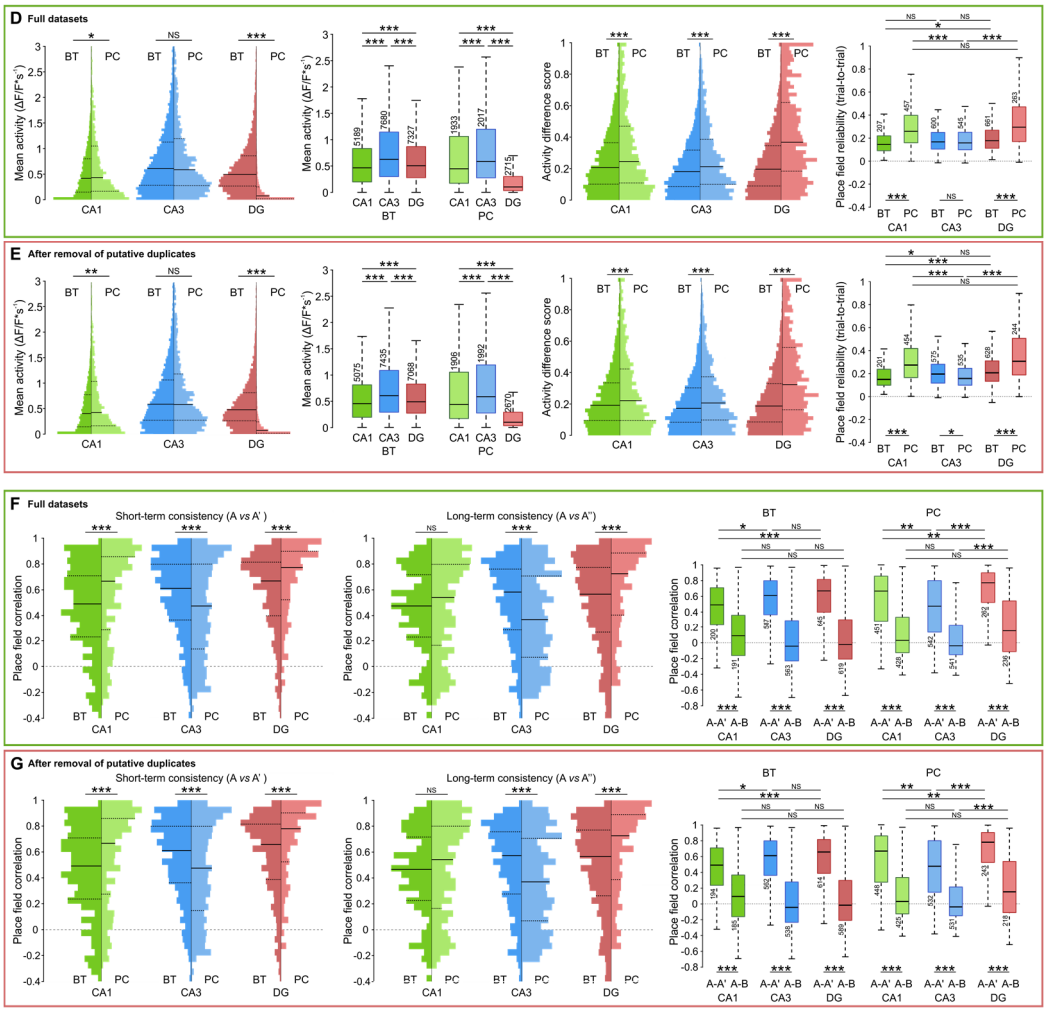

(**A**) Distributions of the maximum activity correlation value of each cell or bouton when compared with all the cells / boutons recorded simultaneously (during the same session) in context A. Using all the cells combined (top left) as the population of reference, we defined the threshold for putative duplicates as 2σ (standard deviation) above the mean value of the fitted Gaussian density curve (μ), which corresponds to a correlation value of 0.88. Orange solid line, fitted Gaussian curve; central dotted line, mean value (μ); side dotted lines, limits of the confidence interval (μ ± 2σ); pink area, cells / boutons showing a correlation value above the threshold (i.e. considered as putative duplicates). Top left, all cells; top right, all boutons; rows 2 to 4, left, principal cells in CA1, CA3 and DG, respectively; rows 2 to 4, right, boutons in CA1, CA3 and DG, respectively.

(**B**) Top, raw calcium traces of two cells showing a low correlation of their activity (R = 0.13); bottom, raw calcium traces of two cells showing a high correlation of their activity (R = 0.94).

(**C**) Number of cells and boutons before and after removal of the putative duplicates in each dataset. The thresholding method described in **A** was used to remove putative duplicates based on the activity in context A, then the same approach was applied to remove putative duplicates based on the activity in context B.

(**D**) Using full datasets: left and center-left, mean calcium activity for all boutons (BT) and principal cells (PC). Center-right, activity-rate difference scores (see **STAR Methods**) between contexts A and B. Right, mean trial-to-trial reliability of place BT and PC in context A.

(**E**) Same as **D** after removal of putative duplicates.

(**F**) Using full datasets: left and center, mean activity correlations between first and second blocks of runs (left) and first and third blocks of runs (center) in context A; comparison between place BT and place PC for each hippocampal region. Right, mean activity correlations between first and second blocks of runs in context A (A-A') and first block in A and first block in B (A-B) of place BT (left) and place PC (right).

(**G**) Same as **F** after removal of putative duplicates.

D-G, Violin plots: Rank Sum-Tests, per region (CA1 / CA3 / DG). Whisker plots: ANOVA on ranks, Dunn's test, per functional domain (BT / PC). Values represent number of BTs / PCs. NS, not significant; *$p < 0.05$; **$p < 0.01$; ***$p < 0.001$. For exact p values see **Table S1**.

Figure S12 | Alternative transients identification method using only the onsets (rising phases) of the transients and comparison with the classical transients extraction method (full transients, as in the main paper), related to Figures 1-3 and STAR Methods.

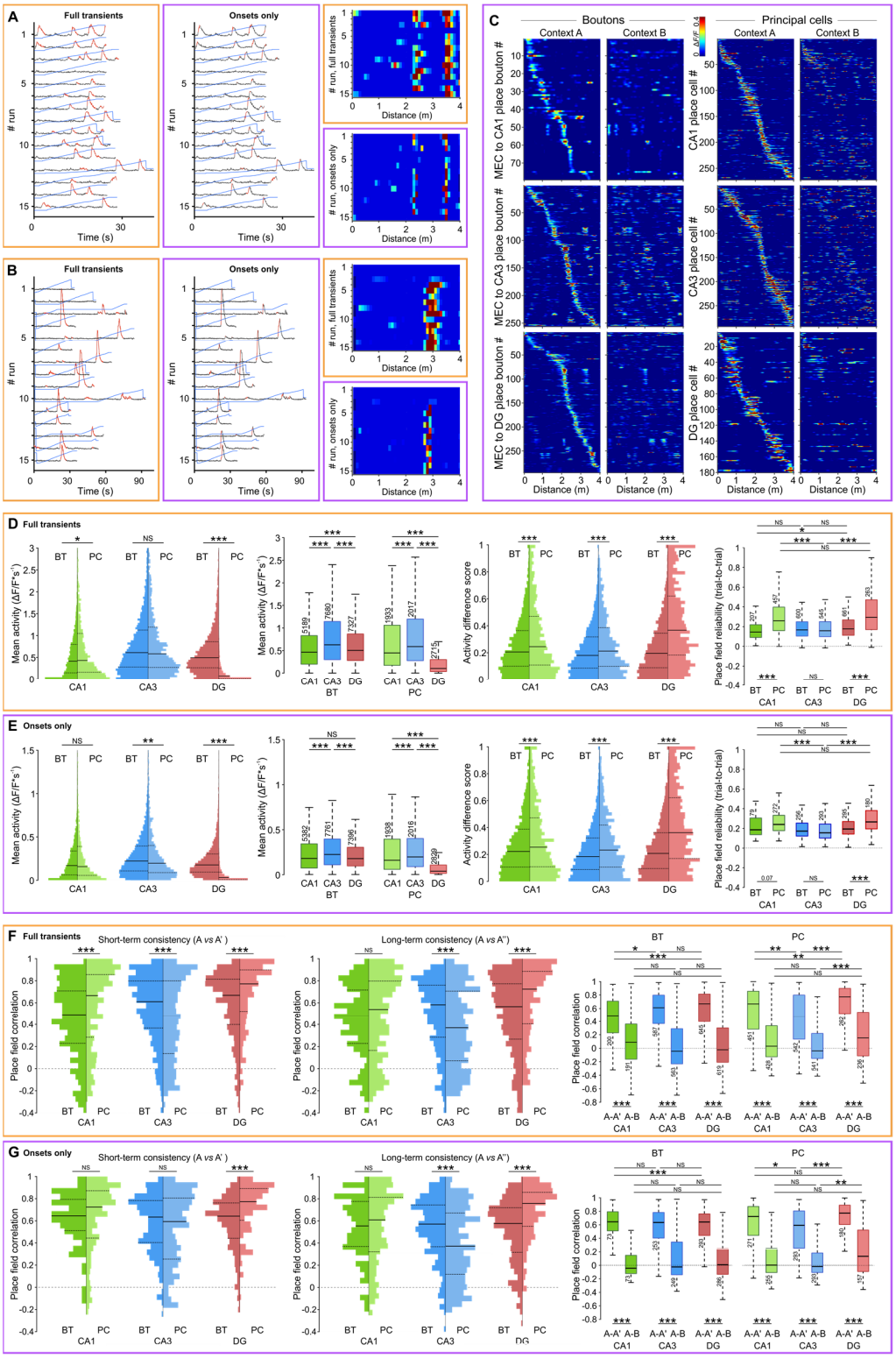

Orange boxes show results obtained with the classical transients extraction method (full transients), while purple boxes show results based on the onsets-only approach.

(**A**) Left, raw calcium traces (grey) with full significant transients (red) as identified in the main paper and linear-track position (blue) over time of a MEC-to-CA3 bouton showing place fields; center, raw calcium traces of the same bouton showing the significant transients (red) as identified using the onsets-only approach. Right, calcium activity over track distance of the same bouton using classical (top) and onsets-only (bottom) transients' extraction methods.

(**B**) Same as **A** for a MEC-to-DG bouton.

(**C**) Left, activity maps of MEC-to-CA1 (top), -CA3 (middle) and -DG (bottom) place-modulated boutons as identified in context A using onsets-only method; right, activity maps of CA1 (top), CA3 (middle) and DG (bottom) place-modulated principal cells as identified in context A using transient onsets-only method.

(**D**) Results using the classical transients' extraction method: left and center-left, mean calcium activity for all boutons (BT) and principal cells (PC). Center-right, activity-rate difference scores (see **STAR Methods**) between contexts A and B. Right, mean trial-to-trial reliability of place BT and PC in context A.

(**E**) Same as **D** using onsets-only transients.

(**F**) Results using the classical transients extraction method: left and center, mean activity correlations between first and second blocks of runs (left) and first and third blocks of runs (center) in context A; comparison between place BT and PC for each hippocampal region. Right, mean activity correlations between first and second blocks of runs in context A (A-A') and first block in A and first block in B (A-B) of place BT (left) and PC (right).

(**G**) Same as **F** using onsets-only transients.

D-G, Violin plots: Rank Sum-Tests, per region (CA1 / CA3 / DG). Whisker plots: ANOVA on ranks, Dunn's test, per functional domain (BT / PC). Values represent number of BTs / PCs. NS, not significant; *$p < 0.05$; **$p < 0.01$; ***$p < 0.001$. For exact p values see **Table S1**.

Figure S13 | Boutons and principal cells with place-fields in both contexts show higher place-field correlations in the DG and CA1 compared to CA3, while MEC boutons in all hippocampal areas show high levels of remapping, related to Figure 3.

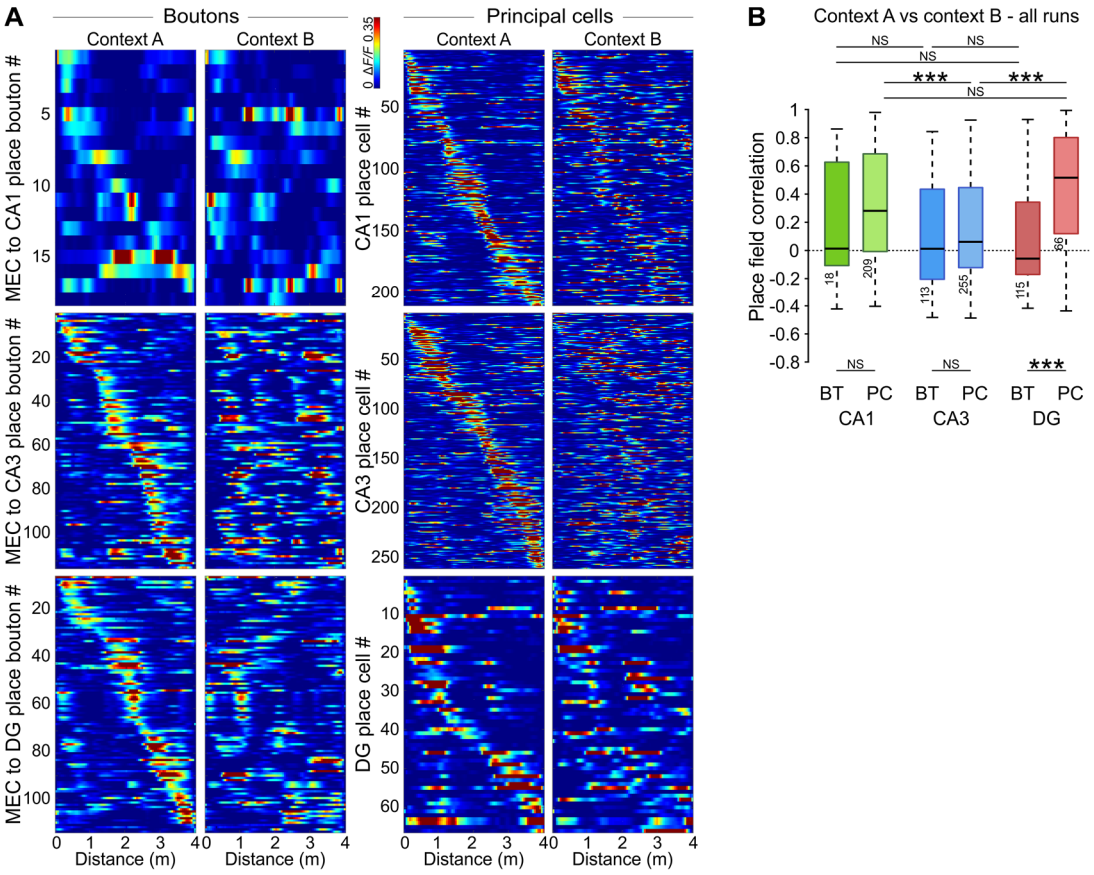

(**A**) Left panel, activity maps of MEC-to-CA1 (top), -CA3 (middle) or -DG (bottom) boutons having place-fields in both contexts. Left column, activity in context A; right column, activity in context B. Right panel, similar to left panel for CA1 (top), CA3 (middle) and DG (bottom) principal cells.

(**B**) Mean activity correlations between all runs in contexts A and B of MEC boutons (BT) and principal cells (PC) having place-fields in both contexts. ANOVA on ranks, Dunn's test. Values represent number of BTs / PCs. Boxes, 25th to 75th percentiles; bars, median; whiskers, 99% range. NS, not significant; ***$p < 0.001$. For exact p values see **Table S1**.

Figure S14 | Stability measures of boutons and cells calcium imaging data, related to Figures 1, S3 and STAR Methods.

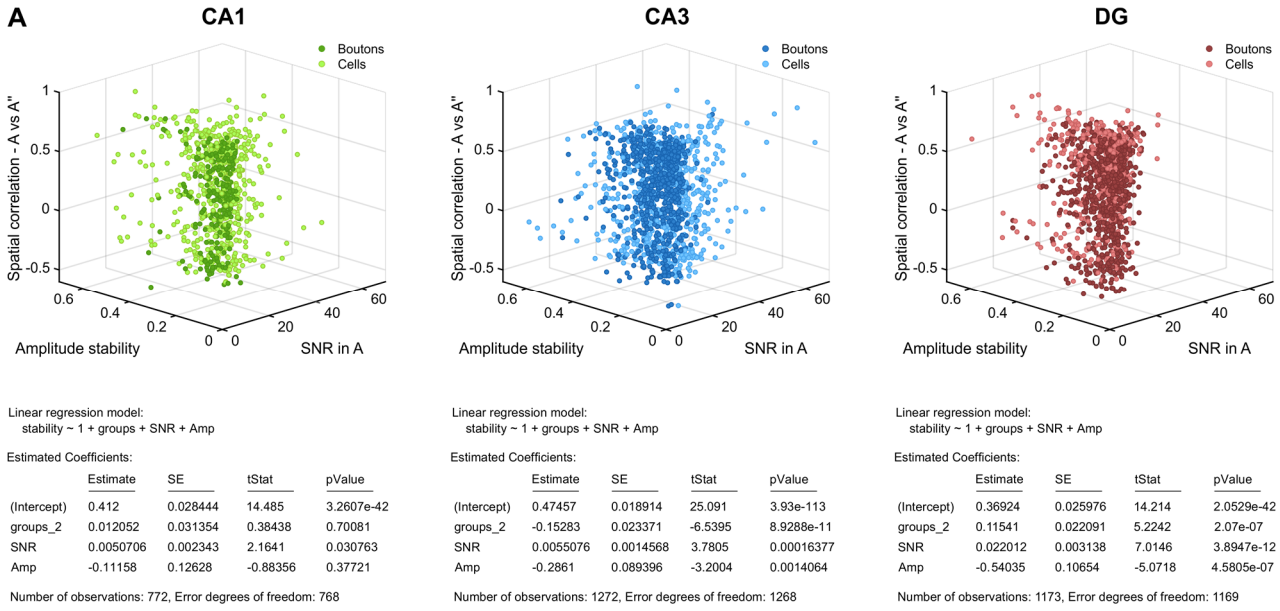

Linear regression model:
stability ~ 1 + groups + SNR + Amp

Estimated Coefficients:

	Estimate	SE	tStat	pValue
(Intercept)	0.412	0.028444	14.485	3.2607e-42
groups_2	0.012052	0.031354	0.38438	0.70081
SNR	0.0050706	0.002343	2.1641	0.030763
Amp	-0.11158	0.12628	-0.88356	0.37721

Number of observations: 772, Error degrees of freedom: 768

Linear regression model:
stability ~ 1 + groups + SNR + Amp

Estimated Coefficients:

	Estimate	SE	tStat	pValue
(Intercept)	0.47457	0.018914	25.091	3.93e-113
groups_2	-0.15283	0.023371	-6.5395	8.9288e-11
SNR	0.0055076	0.0014568	3.7805	0.00016377
Amp	-0.2861	0.089396	-3.2004	0.0014064

Number of observations: 1272, Error degrees of freedom: 1268

Linear regression model:
stability ~ 1 + groups + SNR + Amp

Estimated Coefficients:

	Estimate	SE	tStat	pValue
(Intercept)	0.36924	0.025976	14.214	2.0529e-42
groups_2	0.11541	0.022091	5.2242	2.07e-07
SNR	0.022012	0.003138	7.0146	3.8947e-12
Amp	-0.54035	0.10654	-5.0718	4.5805e-07

Number of observations: 1173, Error degrees of freedom: 1169

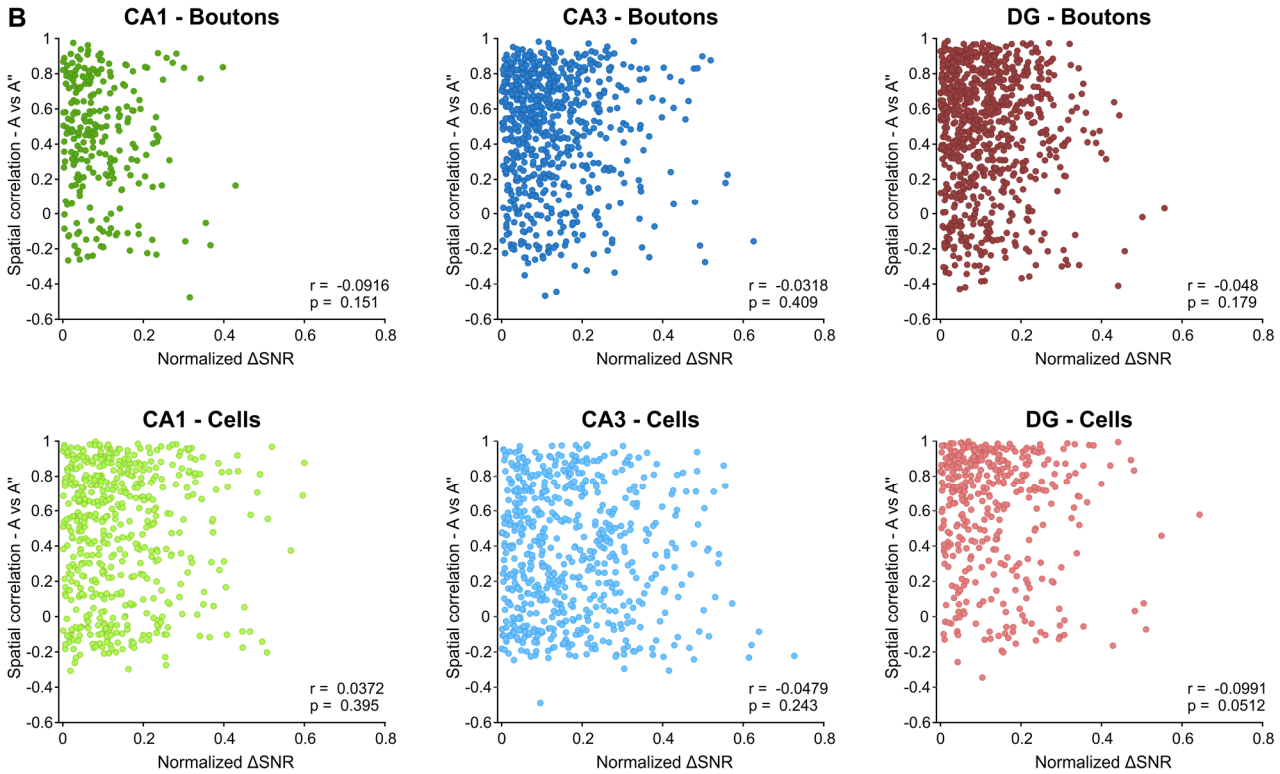

(A) Stability measures are not biased by differences in SNR or amplitude levels between boutons and cells. For each bouton or cell having one (or more) place field(s) in context A, the Signal-to-Noise Ratio (SNR) was defined as the mean amplitude of significant transients divided by the standard deviation of the baseline fluorescence, and the amplitude stability as the absolute difference between the mean transients amplitude in the first (A) and last (A'') blocks of 5 runs in this context, divided by their sum: $|Amp_{A} - Amp_{A''}| / (Amp_{A} + Amp_{A''})$. Spatial stability was calculated as the correlation between the same blocks of runs (A vs A'', also referred as long-term consistency, see **STAR Methods**). *Top part*, 3D scatter plots with the spatial correlation between A and A'' (Y-axis) plotted against the SNR in A (Z-axis) and amplitude stability (X-axis). Left, CA1; center, CA3; right, DG. Boutons, dark-colored dots; cells, light-colored dots. *Bottom part*, summary of a linear regression model with spatial stability (spatial correlation – A vs A'') as the response variable and the other variables (group (boutons or cells), SNR in A, and amplitude stability) as the predictor variables, for the CA1 (left), CA3 (center) and DG (right) boutons and cells populations plotted above. Abbreviations: Estimate, coefficient estimates for each corresponding term in the model; SE, standard error of the coefficients; tStat, t-statistic for each coefficient (tStat = Estimate/SE); pValue, p-value for the t-statistic; Number of observations, number of boutons and cells considered; Error degrees of freedom, n - p, where n is the number of observations, and p is the number of coefficients in the model.

(B) Variations in the Signal-to-Noise Ratio over time do not influence long-term consistency. For each bouton / cell having place field(s) in context A, the SNR was calculated for the first block of 5 runs (SNR_{A}) and for the last block of 5 runs ($SNR_{A''}$) in this context. Normalized Signal-to-Noise Ratio change (ΔSNR) was defined as the absolute difference between these two SNR measures, divided by their sum: $\Delta SNR = |SNR_{A} - SNR_{A''}| / (SNR_{A} + SNR_{A''})$. To exclude any influence of the variation of the SNR onto spatial stability measures, we inspected whether the ΔSNR and the spatial correlation between the first and last blocks of 5 runs (A vs A'') scale together. No dependence was observed, regardless of the area (CA1, CA3 and DG) and population (boutons, cells) considered. *Top row*, MEC boutons recorded in CA1, CA3 and DG, respectively; *bottom row*, PCs recorded in CA1, CA3 and DG, respectively.

Figure S15 | Details of decoding approach and additional data, related to Figure 4.

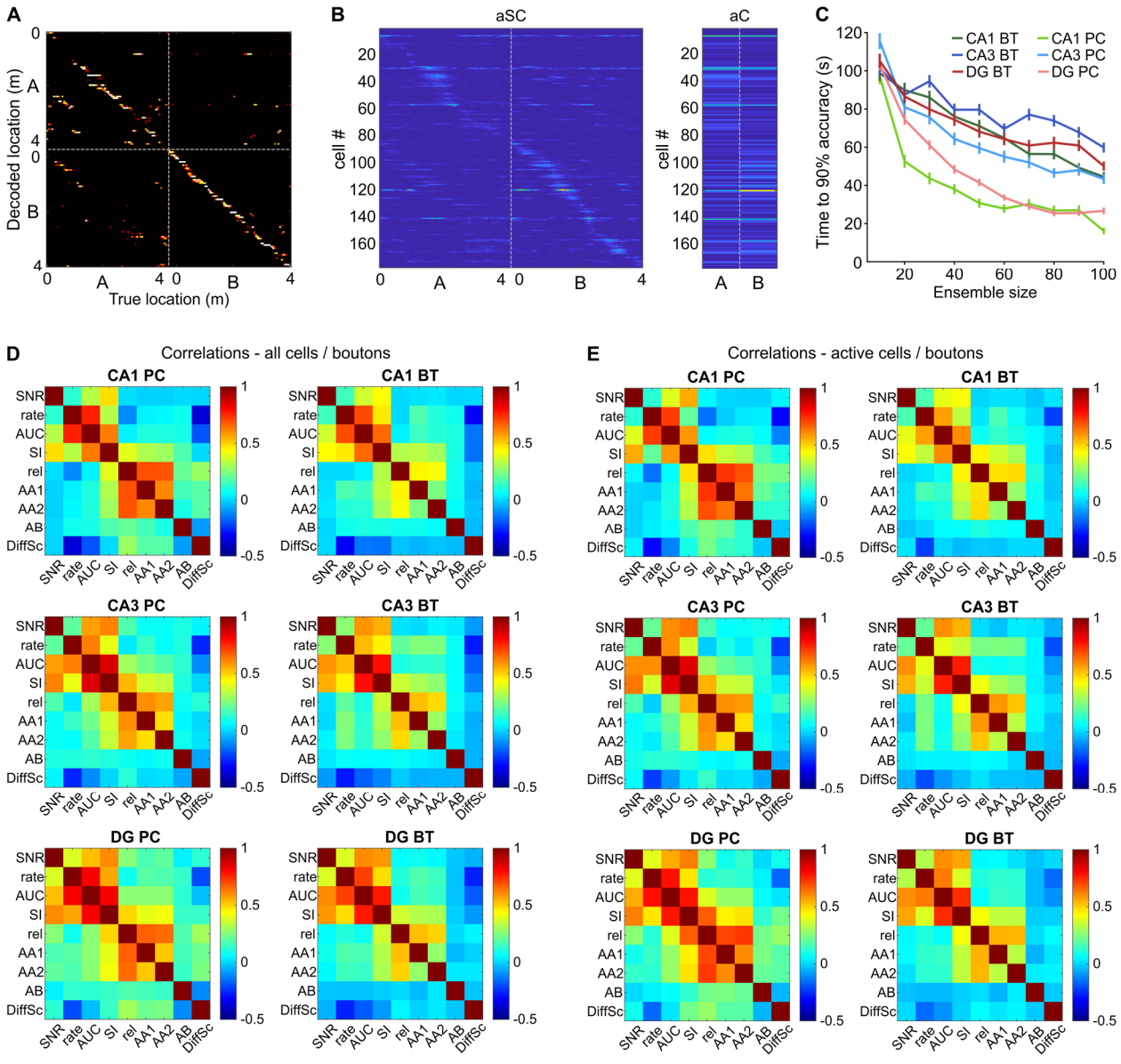

(**A**) Illustrative example of a confusion matrix of actual mouse location (x-axis) and maximum-likelihood decoded locations (y-axis). Dotted boxes (upper left, lower right) outline real location in context A or B, respectively.

(**B**) Illustrative example of the different templates used for the decoding approach in **Figure 4G**. Templates were constructed either from the context-specific spatial activity patterns (aSC, left) or by using only the mean activity rates for each context (aC, right). Example shows templates obtained from a dataset of 177 CA1 pyramidal cells.

(**C**) Mean time to 90% context-decoding accuracy over ensemble size for cells (light colours) and MEC boutons (dark colours) in the various hippocampal areas.

(**D**) Correlation (Pearson's R) between spatial activities related parameters for all cells or boutons, respectively, in the individual hippocampal subfields. *Abbreviations*: *SNR*, signal-to-noise ratio; *AUC*, calcium signal (AUC) over time; *SI*, spatial information; *rel*, trial-to-trial reliability; *AA1*, A-A' place field correlation (short-term consistency); *AA2,* A-A" place field correlation (long-term consistency); *AB*, A-B place field correlation (across-context similarity); *DiffSc*, activity-rate difference score between contexts.

(**E**) Same as in **D**, but for active (>2 transients / minute) cells or boutons only, respectively.

For exact p values see **Table S1**.

Figure S16 | CA2 pyramidal cells show intense GCaMP6s expression (as compared with CA3 pyramidal cells), a property that can be used to identify them during in vivo imaging, related to Figure S3 and STAR Methods.

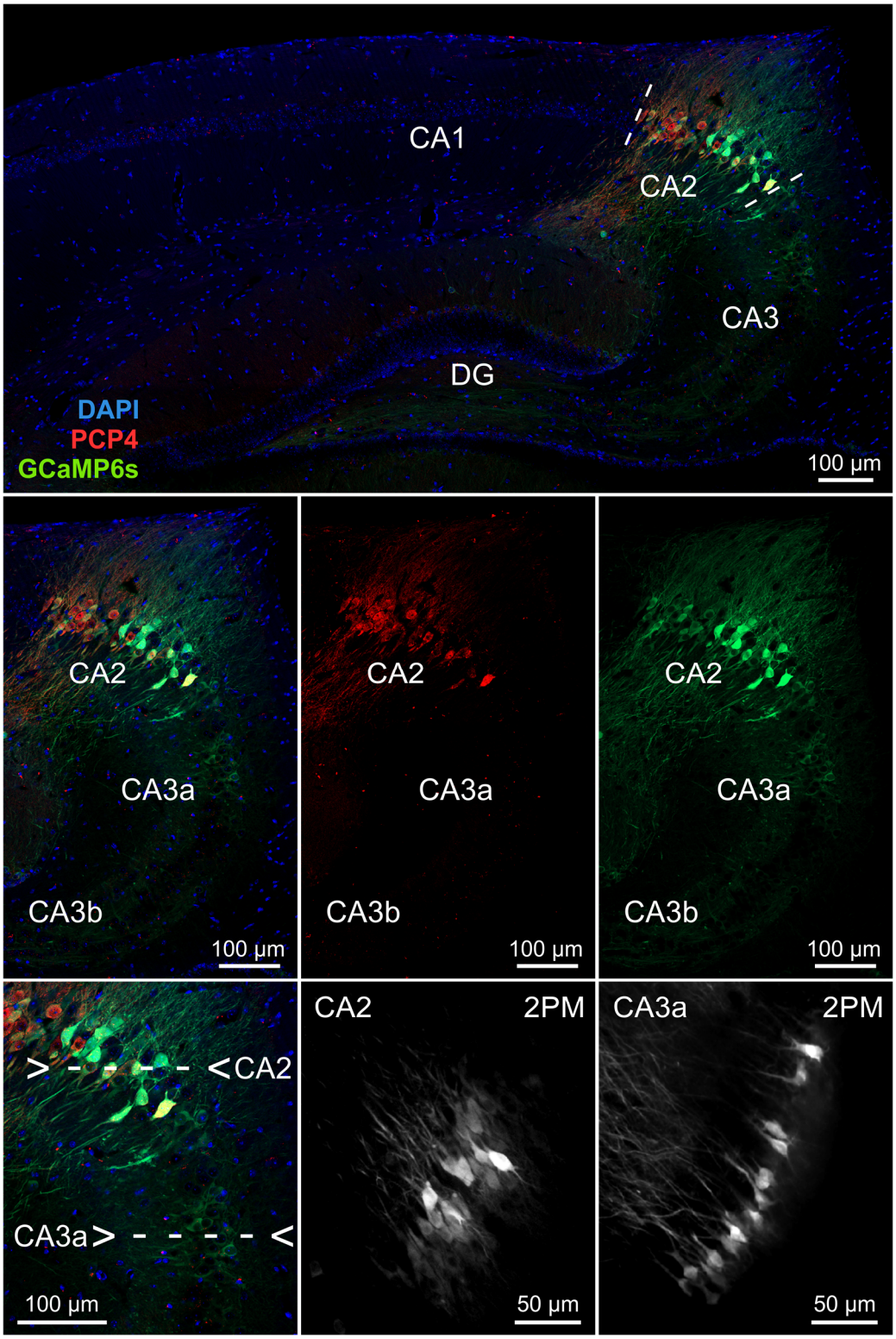

Top panel, sagittal section through the dorsal hippocampus of an animal in which we recorded CA3 principal cells. PCP4 immuno-labeling (see **STAR Methods**) reveals CA2 pyramidal cells in red, GCaMP6s-labeled cells are visible in green, tissue counterstained with DAPI (blue).

Center panel, focus on the region comprising CA2, CA3a and CA3b: left, image obtained using the 3 channels (GCaMP6s / PCP4 / DAPI); middle, PCP4 immunolabeling only; right, GCaMP6s only.

Bottom panel, left, higher magnification of the same sagittal section showing the imaging planes corresponding to CA2 and CA3a (top and bottom dotted lines, respectively); note how the CA3 pyramidal cells appear to be dimly labeled with GCaMP6s as compared to their CA2 counterparts. Middle and right, in-vivo two-photon microscopy images of CA2 and CA3a, respectively (corresponding to the locations indicated by the dotted lines on the left figure).

Figure S17 | Boutons ROIs as identified using Suite2p in CA1, CA3 and DG and examples of calcium signal (3-frames averaged images and raw traces) obtained from MEC-to-Hip boutons, related to STAR Methods.

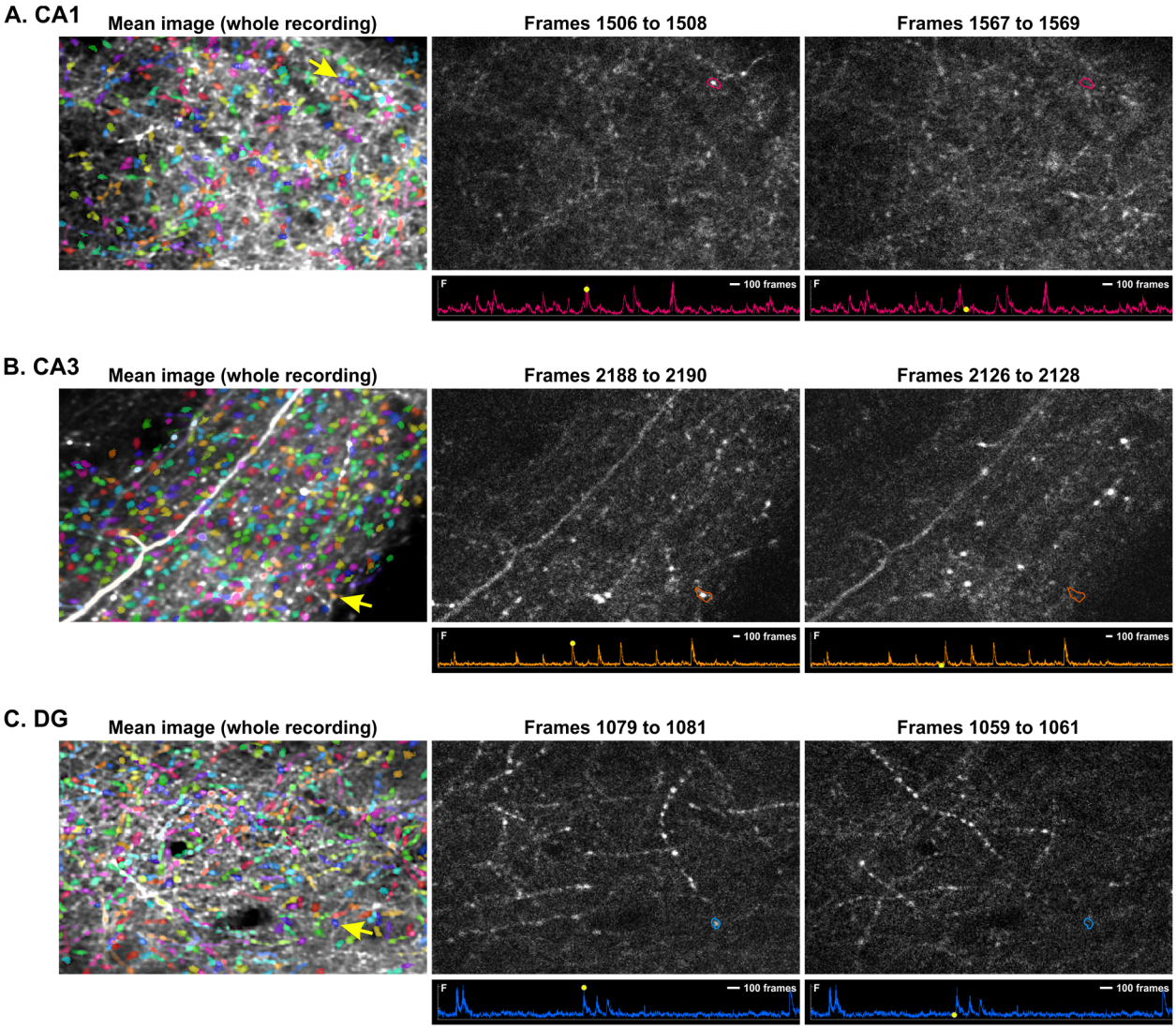

(**A**) Left, mean image of all calcium signals acquired over one entire imaging session. Each colored ROI is representing one bouton (based on Suite2p segmentation algorithm, see **STAR Methods**). Yellow arrow is pointing at one example of a bouton highlighted in center and right panels. Center top, mean image of a 3-frames sequence recorded while this bouton was active. Center bottom, raw calcium trace of this bouton. The yellow circle indicates the moment of the trace corresponding to the image above. Right, same as the center part for a 3-frames sequence recorded while the highlighted bouton was inactive (baseline level). (**B**) and (**C**) Same as **A** for CA3 and DG, respectively.